Identification of defects in piles with high slenderness ratios using dynamic response to impulse loads

Javier Ignacio Ezeberry

IDOM,
Avda. Monasterio de El Escorial 4 – 28049 Madrid, Spain
E-mail: jiezeberry@yahoo.com.ar

Daniel Ambrosini*

Facultad de Ingeniería,
Centro Universitario,
National University of Cuyo,
CONICET,
Parque Gral, San Martín, 5500, Mendoza, Argentina
Fax: +54-261-4380120
E-mail: dambrosini@uncu.edu.ar
*Corresponding author

Abstract: The main objective of this paper is to evaluate the capabilities of the non-destructive impact-response method in detecting the existence of defects in piles with high slenderness ratio. The impact-echo technique was developed many years ago for non-destructive detection of defects in piles and structures. However, it is recognised that this method could be applied confidently for piles with length/diameter relationship up to 20. In the last years, with the development of hardware in computers and sensors, it is now possible to use this method for piles with high slenderness ratio. In this paper, piles of length/diameter relationship of about 40 are studied. A numerical-experimental study was carried out. It was shown that the results of the experiment were in agreement with those of the numerical studies and the accuracy of the impact-echo method was influenced by the type, size and location of the defects. Taking into account the uncertainties related to the studied problem, the obtained results preliminarily allow consider this NDT methodology as a promissory alternative to detect defects in piles with high slenderness ratio.

Keywords: non-destructive testing; pre-cast piles; cast in place piles; finite element model; impact echo technique; high slenderness ratio.

Reference to this paper should be made as follows: Ezeberry, J.I. and Ambrosini, D. (2014) 'Identification of defects in piles with high slenderness ratios using dynamic response to impulse loads', *Int. J. Lifecycle Performance Engineering*, Vol. 1, No. 4, pp.335–356.

Biographical notes: Javier Ignacio Ezeberry obtained his degree in Civil Engineering (2001) at University of Centro (Argentina) and his MSc degree (2003) in the Structures Institute at the University of Tucuman (Argentina). During the period 2004–2009, he works as a Research Assistant in the Structures Laboratory of the Polytechnic University of Madrid (Spain), making focus in the service behaviour of the RC structures. He received a new Master degree in the field of the advanced design of structures in 2011. In the professional field, he works during the period 2004–2007 in the consultancy FHECOR as Project Engineer in Madrid. From January of 2010, he works in IDOM, in the company IDOM, in the field of advanced analysis and the nuclear services.

Daniel Ambrosini is a Full Professor in the Engineering Faculty at the University of Cuyo (Argentina) since 2003. He holds a degree in Civil Engineering (1986) from the same university and MSc (1991) and Dr. Eng. (1994) degrees in the Structures Institute at the University of Tucuman (Argentina). He is a member of the National Academy of Engineering (Argentina), Director of the Structural Engineering Master Program (University of Cuyo), Senior Researcher (CONICET, Argentina) and Head of the Experimental Dynamics Division (University of Cuyo). In 2001 and 2005, he was awarded from the National Academy of Engineering (Argentina) because his trajectory until 40 years and due to the better scientific contribution in 2005. His current research interests include structural dynamics, seismic, blast and wind loadings, control of vibration, structural damage, structural health monitoring (SHM), and nanotechnologies.

This paper is a revised and expanded version of a paper entitled ‘Long piles integrity trough impact echo technique’ presented at the VIII Congreso Argentino de Mecánica Computacional MECOM2005, Buenos Aires, Argentina, November 2005.

1 Introduction

Many civil structures such as buildings, bridges, towers, dams and other massive structures sometimes need special foundations using piers and piles, built alternatively with pre-cast and cast in place techniques. In the first case, the piles may be damaged under the pile driving impact process, in which long and deep cracks may appear. On the other hand, ‘necks’ or ‘bulbs’ may be created in the process of drilling. In both cases, these defects may affect considerably the bearing capacity of the piles.

The importance of assessing the actual quality of a pile foundation has been long recognised. To achieve this goal, various kinds of destructive (load tests) and non-destructive tests were developed. In this aspect, non-destructive testing (NDT) was considered to possess high potential for application because it is featured as cost-effective, damage-free, time-saving and thus can cover the whole population to avoid the disadvantages of sampling and destruction of the piles tested.

Many researchers have been working on the NDT of piles. Most of the tests could be classified into two categories, i.e.;

1 reflection

2 direct transmission methods (Liao et al., 2006).

Among others, tests as categorised in reflection methods could be impulse response (IR) (Davis, 2003; Liao and Roesset, 1997a, 1997b) or transient dynamic response (TDR) (Davis and Dunn, 1974), sonic echo (SE) (Rausche et al., 1992), impedance log (IL) (Paquet, 1991; Rix et al., 1993), receptance theory (Lilley, 2000) and impact echo (IE) (Lin et al., 1997; Kim et al., 2002; Masoumi et al., 2009). Tests, as categorised in direct transmission methods, could be cross-hole sonic logging (CSL), gamma-gamma testing method, accoustic emission (AE) (Luo et al., 2004; Shah and Ribakov, 2010), optical fibre (OF) (Li et al., 2004; Kister et al., 2007) and parallel seismic (PS) (Liao et al., 2006; Niederleithinger, 2012). In reflection methods, the force to introduce a disturbance to a pile and the receiver to collect the response of the pile are basically applied at the pile head, whereas in direct transmission methods the receiver is placed at intervals in a tube or a borehole which must be cored or drilled before being tested. Therefore reflection methods are in general faster and more cost-effective. However, direct transmission methods can obtain the information in a more direct way and they can be applied to piles with much larger length (Liao et al., 2006). Finally, it must be mentioned a class of methods that analyse the response and capacity of piles while they are being driven in the soil. This method is normally named CASE method (Rausche et al., 1985). Duan and Oweis (2005) used dyadic wavelet transform to analyse PDA measured signals in order to identify the CASE-damping factor.

In connection with theoretical and numerical studies, most papers used 1D model however, some authors presented more sophisticated models. Lin et al. (1997) who conducted analyses of piles using the DYNA2D and DYNA3D codes, Liao (1994) compared 1D, 2D and 3D models. Rao and Rao (1999) studied pile machine foundations in the time domain using the Lanczos vectors in 3D FEM models. Liao and Roesset (1997a) analysed the dynamic response of intact piles to impulse loads. They showed that the 3D model results are very similar, in general terms, to those predicted by the usual 1D solution. Palacz and Krawczuk (2002) introduced a new finite spectral element of a cracked rod for damage detection. Ni et al. (2008) combine continuous wavelet transform (CWT) method with SE method. Finally, related with this paper, Ni et al. (2006) developed a joint time–frequency analysis to study the integrity of a pile with a slenderness ratio of 38.6 and Tenenbaum et al. (2011) studied the damage influence on the vibrational behaviour and on the wave propagation issues of a slender Euler-Bernoulli beam.

Recently, Prendergast et al. (2013) examined the effect of scour on the vibration characteristics of piles using laboratory and field testing and Hess et al. (2014) studied the characteristic features and applications of linear and nonlinear guided elastic waves propagating along surfaces (2D) and wedges (1D) and reviewed laser-based excitation, detection, or contact-free analysis of these guided waves with pump–probe methods.

The impact-echo technique, based on the use of transient elastic waves was developed many years ago for non-destructive detection of defects in piles and structures. Moreover, is recognised in the specialised literature that this method could be applied confidently for piles with length/diameter relationship up to 20 (Davis and Dunn, 1974) or 30 (Lilley, 2000). However, with the development of hardware in computers and new sensors and dynamic equipment, it is now possible to explore the use of this method for piles with high slenderness ratio. In this paper, piles of length/diameter relationship of about 40 are studied. Moreover, experimental tests are used to calibrate the numerical model and evidence is presented about the importance of the soil in the global damping and spread

of the waves propagating along the pile. Taking into account the uncertainties involved in the physical problem studied and the limits of the proposed approach, the obtained results preliminarily allow consider this NDT methodology as a promissory alternative to detect defects in piles with high slenderness ratio. Finally, some useful recommendations about frequency filters and sensors are drawn.

2 Problem definition

IE techniques involve the introduction of a transient stress pulse into a test object by a mechanical impact with a hammer and monitoring the surface displacements, velocities or accelerations caused by the arrival of reflections of the pulse from internal defects and external boundaries (Figure 1). The pulse consists of stress waves (compression stress waves) propagating along the body of the bar by spherical wave-fronts. If on the way down impedance variations are encountered (e.g., as a results of changes in the cross sectional area, cracks, variations in soil layers, or inclusions of foreign material), some or all of it may propagate into the new medium or be reflected from it. The part that enters the new medium is called the transmitted portion and the other the reflected portion. If the incident medium has a lower index of refraction then the reflected wave has a 180° phase shift upon reflection. Conversely, if the incident medium has a larger index of refraction the reflected wave has no phase shift. When the wave enters to a new medium, the speed of propagation will change. In order to match the incident and transmitted wave at the boundary, the transmitted wave will change its direction of propagation. For example, if the new medium has a higher index of refraction, which means the speed of propagation is lower, the wavelength will become shorter (frequency must stay the same because of the boundary conditions).

Figure 1 Physical problem analysed (see online version for colours)

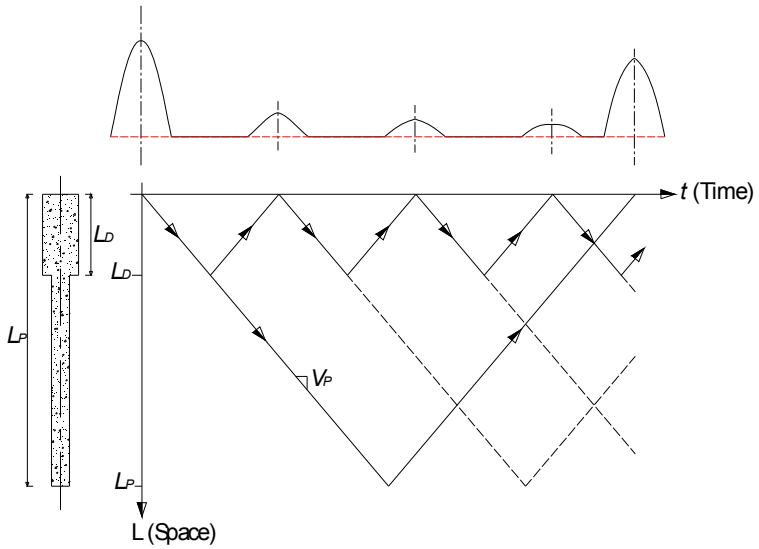

At the top surface, the waves are reflected again and they propagate into the object. In this form, a transient resonant condition is set up by multiple reflections of waves between the top surface and internal flaws and external boundaries. An indefinite reflection occurs only in the abstract case of absence of damping.

A transducer that measures displacement, velocities (geophone) or accelerations (accelerometer) is located close to the impact point and it is used for monitoring the response of the surface caused by the arrival of these reflected waves.

After tests, a numerical model of the piles-soil system must be made and through a dynamic analysis in the time and/or frequency domains the length of piles and possible defects are detected.

3 Dynamic tests

3.1 Experimental set-up and instrumentation

As it was mentioned before, the IR and impact-echo methods use a low-strain impact to send stress waves through the tested element (Figure 2). The device used is usually a hammer with or without a built-in load cell in the hammerhead. The response to the input stress is measured using a geophone or accelerometer. The voltage signals generated by the transducer and eventually by the hammer are normally conditioned and amplified by an amplifier and the resulting signal is sent to a notebook computer for data acquisition and storage (Figure 2). After that, the results are analysed using a numerical model and processing data techniques.

Figure 2 Experimental methodology of impact-echo method

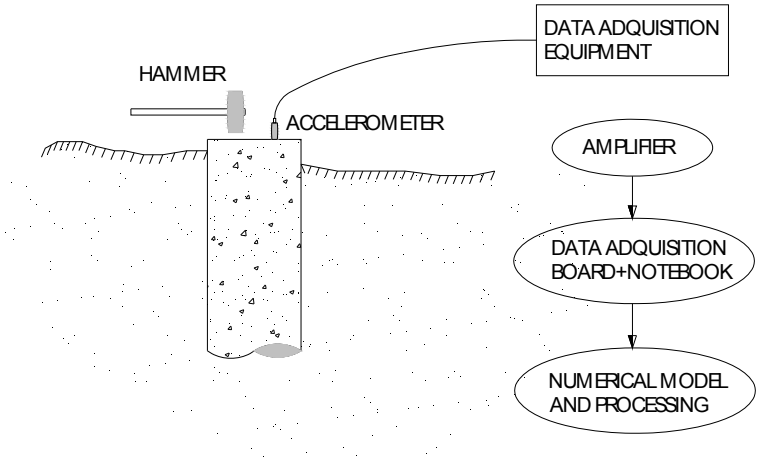

In connection with this paper, it must be noted that the main objective of the tests is to use this experimental results to verify the correctness of the 1-D finite element (FE) model. The following equipments and instruments were used:

Accelerometers KYOWA AS-GB, 100 mV/g sensitivity, were used to measure the dynamic response of the piles. A dynamic strain amplifier KYOWA DPM-612B

amplified the signal generated by the accelerometers. Moreover, the amplifier has a low-pass filter applied to avoid aliasing. A data acquisition board Computerboards PCM-DAS16D/16 of 16 bit of resolution and a maximum conversion time of 10 μs (100 KHz) was mounted on a notebook computer in order to record and process the signals with the programme HP VEE 5.0 (Hewlett-Packard, 1998). The piles were excited with a hammer blow with different head weights from 590 g to 3 kg in order to excite different frequency contents. Rausche et al. (1992) estimates the applied force as 1,000 times the weight of the hammer. On the other hand, Davis (2003), states that typical peak stress levels range from 5 MPa for hard rubber tips to more than 50 MPa for aluminium tips.

The signals were sampled, for all tests, with the following parameters: N = 75,000 (total number of points), n = 15,000 (sampling rate or number of points per second), T = 5 s (total time of the sample), $\Delta t = 6.6710^{-5}$ s, (time interval), Δf = 0.2 Hz (frequency interval), $f_{máx}$ = 1,500 Hz (maximum frequency).

An algorithm to obtain and process the data was programmed in the environment HPVEE. After applying the fast Fourier transform, the spectrum was calculated using the Welch method (Peeters, 2000). The signal processing includes corrections using square minimum techniques, low-pass filter and an Ormsby filter.

3.2 Case study

Pre-cast tube concrete piles were tested both on air (Figure 3) and inserted into the soil. External and internal diameters were 0.33 and 0.19 m respectively and the pile length is 13.27 m giving a length/diameter relationship of approximately 40. The field measured wave velocity was 3706.1 m/s which presents a very low coefficient of variation: 9 10^{-4}. Considering 2,400 kg/m^3 as the mass density of the concrete, an E = 33.0255 GPa elasticity modulus was estimated.

Figure 3 Concrete annular piles tested in CTNOA S.A.

4 Computational model

4.1 Dynamic loading

The dynamic load $p(t)$ used in the analysis was defined as a sinusoidal impact of a duration of half a cycle and a $2T_d$ period:

$$p(t) = \begin{cases} p_0 \sin(\bar{\omega} t) & \text{for } 0 \le t \le T_d \\ 0 & \text{for } t > T_d \end{cases} \quad (1)$$

In a previous paper (Ezeberry et al., 2003), the influence of shape, duration and magnitude of the dynamic load was studied.

4.2 FE model

Although various previous studies (Ezeberry et al., 2003) were performed using 1D and 3D models, the same qualitative conclusions as Liao and Roesset (1997b) were obtained in the sense that the response obtained with the 3D model is very similar in general terms to those predicted by the 1D solution. For this reason, only the results obtained for the 1D model are showed in this paper.

Figure 4 One dimensional model for piles and surrounding soil (see online version for colours)

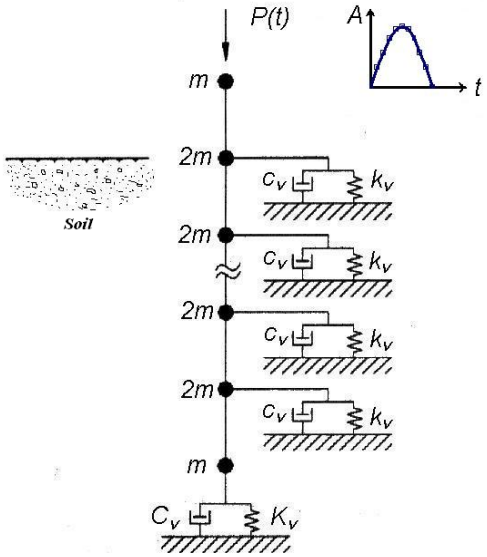

Source: Kim et al. (2002)

The piles were discretised using two-node, isoparametric truss elements in the one-dimensional analysis using standard linear elements under axial deformation, with a linear variation of displacements. A schematic representation of one-dimensional FE model is shown in Figure 4. To simulate the effect of the soil on the lateral surface of the pile, distributed springs with elastic stiffness k_v and dashpots with damping coefficient c_v were applied to each segment below the ground surface. The soil at the base of the pile

was modelled using a spring with elastic constant K_v and a dashpot with the damping coefficient C_v (Liao and Roesset, 1997a). c_v and C_v are intended to represent the radiation (or geometric) damping. The material damping in both pile and soil are assumed to be negligible under low strain integrity testing conditions. The values of the soil parameters per unit length of pile were determined through the following equations (Liao and Roesset, 1997a):

$$k_v = 2.3G_s \tag{2}$$

$$c_v = 2\pi\rho_s V_s r_p \tag{3}$$

$$K_v = 4G_s r_p / (1 - v_s) \tag{4}$$

$$C_v = 0.85K_v r_p / V_S \tag{5}$$

In which the properties of the soil are used: G_s the shear modulus, ρ_s the mass density, v_s the Poisson modulus, V_s the shear wave velocity (S-waves) and r_P the radius of the circular footing, resting on the top of the soil and in this case is equal to the radius of the pile analysed.

Another important factor influencing the results of the FE analysis is the element size. It is shown that in order to obtain a satisfactory result, the element size (Δl) should be less than about one tenth the wavelength (λ) of the highest frequency waves propagating in the shafts (Kim et al., 2002) i.e.;

$$\Delta l \leq \frac{\lambda}{10} \tag{6}$$

4.3 Equations of motion

The dynamic motion equations that govern the physical problem are given by:

$$\mathbf{M}\ddot{\mathbf{U}} + \mathbf{C}\dot{\mathbf{U}} + \mathbf{K}\mathbf{U} = \mathbf{R} \tag{7}$$

in which **M**, **C** and **K** are the mass, damping and stiffness matrix respectively and **R** is the external loading vector; **U**, $\dot{\mathbf{U}}$ and $\ddot{\mathbf{U}}$ are the displacement, velocity and acceleration vector respectively.

Both direct integration and mode superposition methods were used in order to numerically solve the system (7). Both schemes are equivalent but the computational cost is different.

The direct integration is carried out using the Hilbert, Hughes and Taylor method (Bathe, 1996), also named *α method* which is based in the solution of the following modified equation:

$$\mathbf{M}^{t+\Delta t}\ddot{\mathbf{U}} + (1+\alpha)\mathbf{C}^{t+\Delta t}\dot{\mathbf{U}} - \alpha\mathbf{C}^{t}\dot{\mathbf{U}} + (1+\alpha)\mathbf{K}^{t+\Delta t}\mathbf{U} - \alpha\mathbf{K}^{t}\mathbf{U} = (1+\alpha)^{t+\Delta t}\mathbf{R} - \alpha^{t}\mathbf{R} \tag{8}$$

The system (8) could be considered as an improved trapezoidal rule. The α parameter adds a fictitious damping to the model that gives stability to the method by damping strongly the higher modes. The value of α is between 0 and –1/3. When α equals zero, this method is equal to the linear acceleration method [Newmark method, Bathe (1996) with $\beta = 1/4$), but when $\alpha = -1/3$, an important amount of fictitious damping exists.

In the mode superposition method, integration algorithms are used, that assumed a linear variation of temporal functions between the points defined by the temporal increments. This method is extremely efficient in cases in which only few modes are necessaries in order to obtain a right dynamic response.

5 Numerical-experimental comparison

5.1 Piles in the air

In order to validate the experimental procedures and control the proper functioning of equipments, a set of tests with isolated piles in the air were performed. A typical frequency spectrum is presented in Figure 5, in which up to nine peaks could be distinguished associated to the first nine axial vibration modes of the piles.

Figure 5 Frequency spectrum from a test – pile in the air

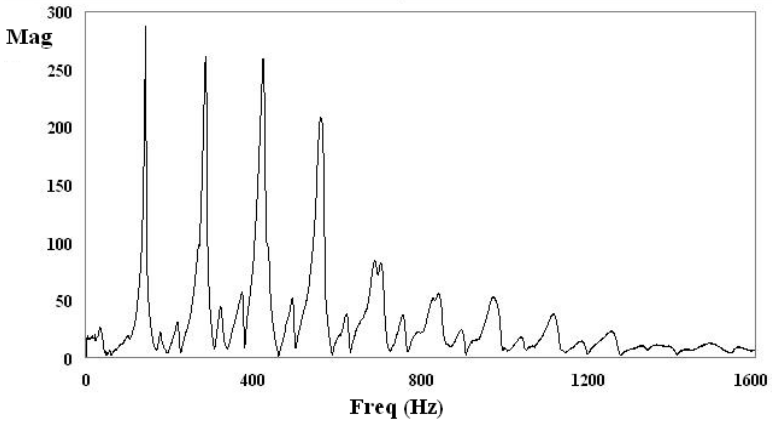

The damping coefficient was determined from the spectrum peaks using the half power bandwidth method. The results obtained are presented in Table 1.

Table 1 Damping coefficients

Mode	*1*	*2*	*3*	*4*	*5*	*6*	*7*	*8*	*9*
ξ	0.012	0.018	0.015	0.014	0.020	0.018	0.013	0.011	0.010

In order to obtain the dynamic response, the impact force was calculated using the value suggested by Rausche et al. (1992) giving to the magnitude of the pulse a value about 6,000 N. After some numerical tests, duration of the pulse of 1.5 ms was selected. The FEM model was built with truss elements of 0.05 m in length. The mode superposition method using the first ten modes was selected in this case in order to solve the system (seven). A temporal increment similar to those used in the field tests was selected ($6.6667\ 10^{-5}$ sec). The numerical-experimental comparison is presented in Figure 6. A very good correlation was founded and the numerical and experimental curves are similar.

The results in this stage were important to verify some parameters of the numerical model, such as pulse, time step, concrete properties etc.

Figure 6 Numerical-experimental comparison. Pile in the air; (a) complete record (b) zoom of the first 16 ms (see online version for colours)

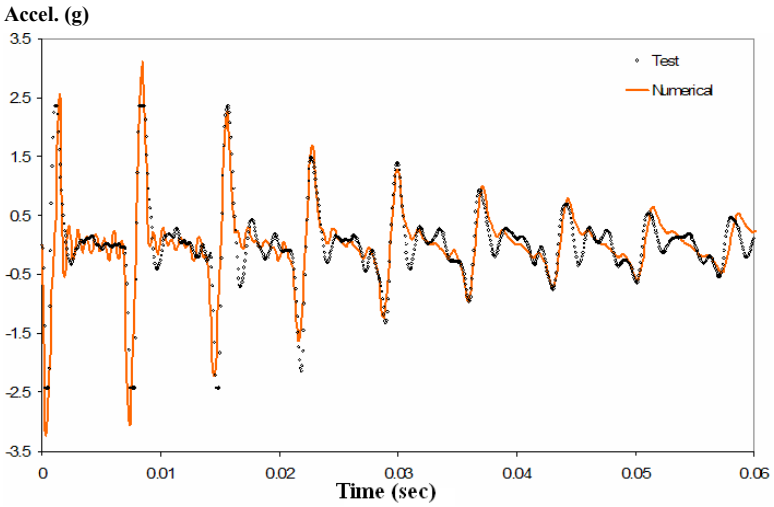

(a)

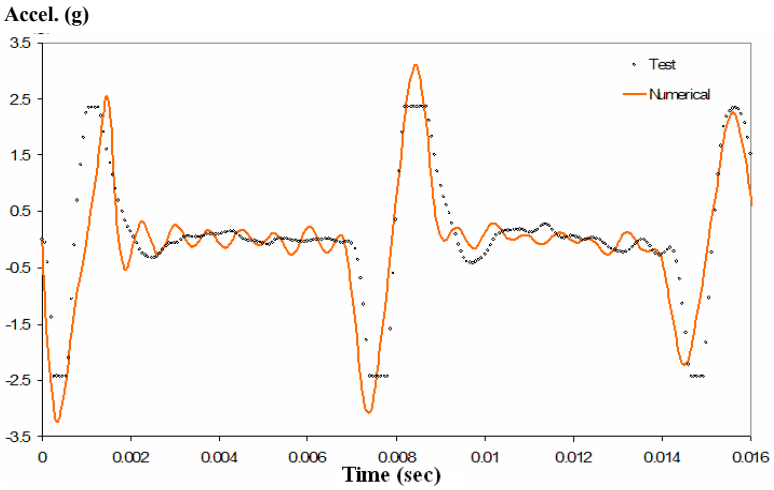

(b)

5.2 Piles inserted into the soil

In order to calibrate the numerical model a comparison between the numerical and experimental responses of piles inserted into the soil was carried out. Then, similar piles that those studied in the air were tested inserted into the soil. When the pile is within the soil, the radiation condition applies and the waves are propagated away from the system pile-soil. The main consequence of this effect is a critical increase in the total damping

and it is much more difficult to detect the reflection of the waves not only in the defect but in the bottom too.

Figure 7 Test results – pile inserted into the soil

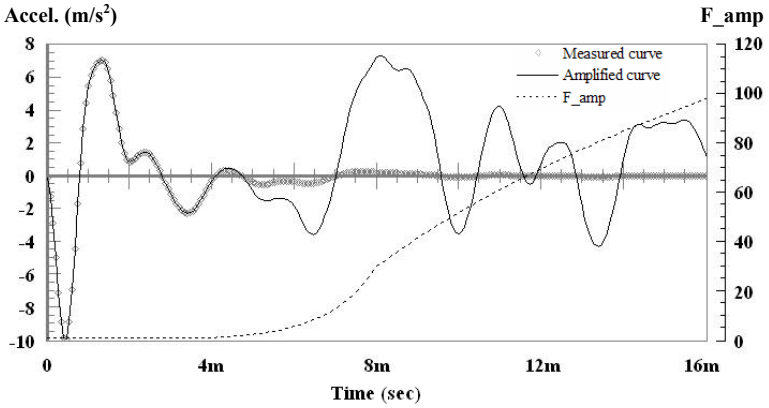

In Figure 7, the tests results are presented in a pile that has a variable free length above the soil between 1.7 and 1.9 m. The mass of the hammer was 3 kg and a 1,500 Hz low-pass filter was applied to the measured data. Only the first 16 ms of the dynamic response is showed because the wave is quickly damped.

In order to distinguish the different reflect waves more clearly, the original measured curve was amplified using an appropriate amplifying function combining constant, exponential and logarithmic functions. With this purpose, a new non-dimensional *proposed* function f_{exp} (**F_amp**) (Ezeberry, 2003) is used to amplify the measured data. Both curves real and amplified are showed in Figure 7. In the amplified curve, the peaks are detected in an easier way.

The *proposed* non-dimensional amplifying function f_{exp} is defined as:

$$f_{exp} = \begin{cases} 1 & 0 \le t \le T_0 \\ b_0 \exp\left(b_1(t)\right) & T_0 \le t \le T_1 \\ b_2 + b_3 \ln(t) & T_1 \le t \le T_2 \end{cases} \tag{9}$$

in which b_0, b_1, b_2 and b_3 and T_0, T_1 and T_2 are determined for each test as described in Ezeberry (2003) by using the following criteria: T_0 is the time until which the response does not have amplification (f_{exp} = 1) and is usually adopted as $T_1/2$; T_1 is the time that corresponds to the 'theoretical' length of the pile and, in this point, the exponential function is replaced by the logarithmic one; and T_2 is the final time until the response needs to be studied. The level of amplification at the T_2 time, $f_{exp}^{T_2}$ is defined arbitrarily taking into account the experimental and numerical tests performed and normally its value is set between 150 and 200. Finally, the level of amplification at the T_1 time, $f_{exp}^{T_2}$ is established as $f_{exp}^{T_2} / N$ in which N is a proposed parameter that is adjusted with the experimental results and equal to 4. Using this data, the values of the unknown parameters b_i are determined by using a least square method for each case. In this case, the following values were used T_0 = 4 ms, T_1 = 8 ms (f_{exp} = 37.5) and T_2 = 20 ms

(f_{exp} = 150). It must be pointed out that the logarithmic function is used for limiting the high grow due to the exponential function, which leads to distortions in the signal.

Figure 8 Numerical-experimental comparison. Pile 1 inserted into the soil

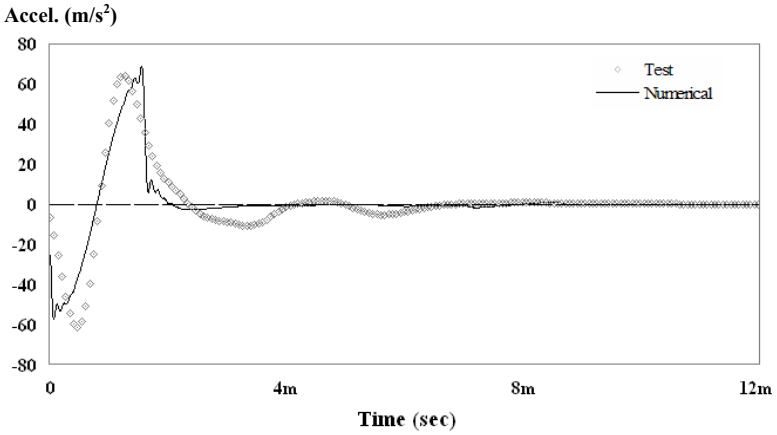

In Figure 8, a numerical-experimental comparison is presented. The soil data were obtained by using the BIG database (Geotechnical Information Bank) from geotechnical parameters for the soils in Tucuman city (Argentina) (Segura, 1993). Then, for the soils at the site, the following parameters were used: $G = 3 \cdot MN/m^2$, $\gamma = 1{,}600$ kg/m^3 and $v_s = 0.2$ for the upper layer (5m) and $G = 8 \cdot MN/m^2$, $\gamma = 1{,}800$ kg/m^3 and $v_s = 0.49$ (soil below the freatic level) for the lower layer. Then, the values for the parameters (2) to (5) are: $k_v = 6.9$ MPa; $c_v = 6.53\ 10^4$ kg/(m sec); for the upper layer and $k_v = 18.4$ MPa; $c_v = 1.13\ 10^5$ kg/(m sec); $K_v = 3.53\ 10^6$ N/m; $C_v = 6{,}750$ kg/sec for the lower layer. The pulse generated for the 3 kg head-hammer was estimated as having a 13,540 N amplitude and a 1.6 ms total duration. The time-step used in the direct integration dynamic analysis was $1 \cdot 10^{-5}$ s. As it was expected, when the pile is inserted into the soil more differences could be appreciated between the results from experimental tests and the numerical ones. As it was mentioned previously, the wave was strongly damped by the soil. The reflection of the wave at the end of the pile (at about 8 ms) cannot be distinguished in both responses.

Figure 9 Numerical-experimental comparison – pile 2 inserted into the soil (see online version for colours)

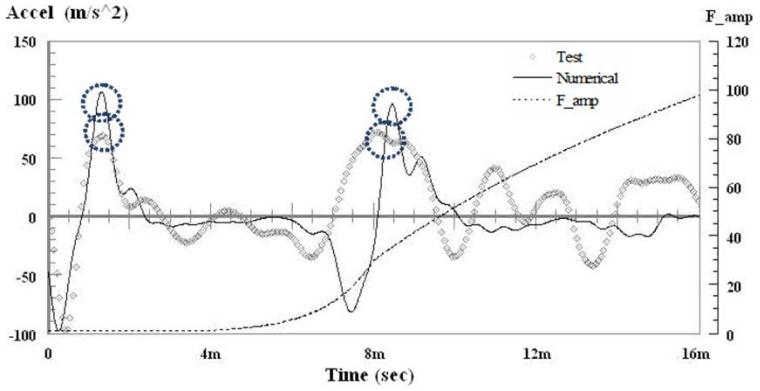

On the other hand, in Figure 9, the dynamic numerical-experimental response of other test is presented. In this figure, the amplification function is applied to both responses. The pulse generated was estimated as having a 23,850 N amplitude and a 1.5 ms total duration.

In spite of some differences observed between measured and numerical responses, the lengths of the pile determined by both responses are similar. In fact, in Figure 9 the peaks to determine the length of the pile are marked with circles. The obtained lengths were: experimental = 12.61 m. numerical = 13.28 m. The obtained difference of 5% seems reasonable considering the uncertainties involved in the problem. Moreover, in other tests lower differences were obtained, of the order of 3% (Ezeberry, 2003). On the other hand, the importance of the amplification function is clearly demonstrated by the results.

6 Identification of defects

6.1 Introduction and hollow-solid cross-section comparison

Considering the main objective of the paper, a numerical study about defects was performed and the results are presented in this section. A model of a pile with equal diameter and length of the test piles was built, but with a solid circular section and a free distance of 0.7 m. The pulse used in the numerical analysis has a 13,540 N amplitude and a 1.6 ms total duration.

Figure 10 Hollow-solid cross-section comparison, (a) 3D hollow model (b) hollow (3D) and solid (1D) responses at different nodes (see online version for colours)

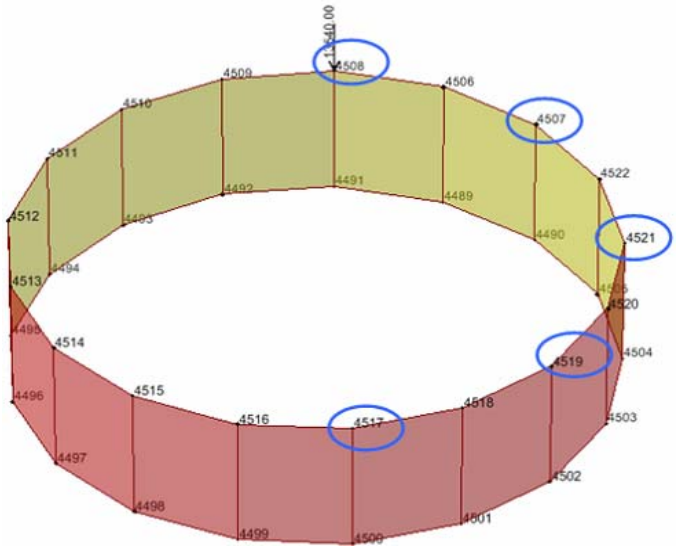

(a)

Figure 10 Hollow-solid cross-section comparison, (a) 3D hollow model (b) hollow (3D) and solid (1D) responses at different nodes (see online version for colours) (continued)

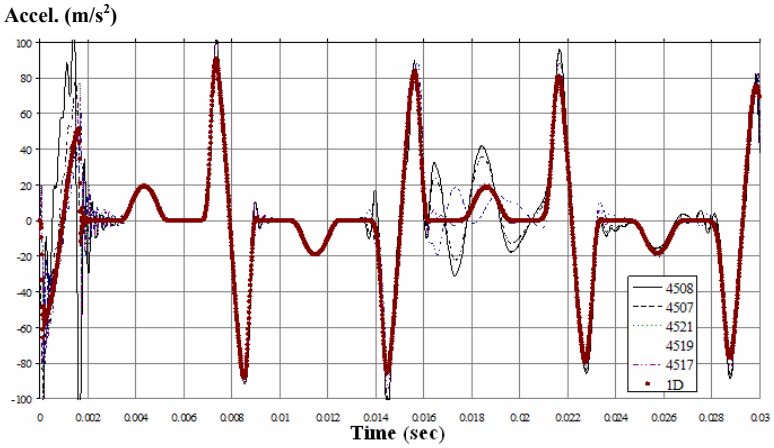

(b)

On the other hand, considering that the numerical 1D model was calibrated by using experimental results from hollow cross-section piles, a comparison study was carried out between the 1D numerical model used in this paper and a 3D numerical model built with shell FEs [see Figure 10(a)] to represent the hollow cross section pile. In Figure 10(b), the responses of 1D and 3D models (in different nodes) are compared. The piles are considered in the air and clamped at the base. It can be seen that, except small differences, the overall response is the same and the same length of the pile could be obtained with both models. Then, the same conclusion was obtained for this case that those obtained by Liao and Roesset (1997a) for 1D and 3D solid models in the sense that the responses are basically the same.

6.2 Neck defects

In this section, a neck defect as presented in Figure 11 is studied. The total diameter (D_p) is reduced 10 cm at a length of 3.25 m from the head of the pile. The neck has a total length (l_c) of 5 cm.

Figure 11 Neck defect

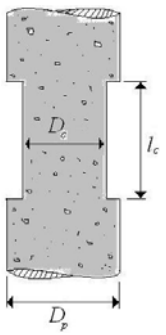

The dynamic response is presented in Figure 12 when a 1,500 Hz low-pass filter is used. Moreover, the Figure 13 shows the dynamic response when an 8,000 Hz low-pass filter is used.

Figure 12 Numerical analysis. Neck defect. 1,500 Hz low-pass filter. Location: 3.25 m

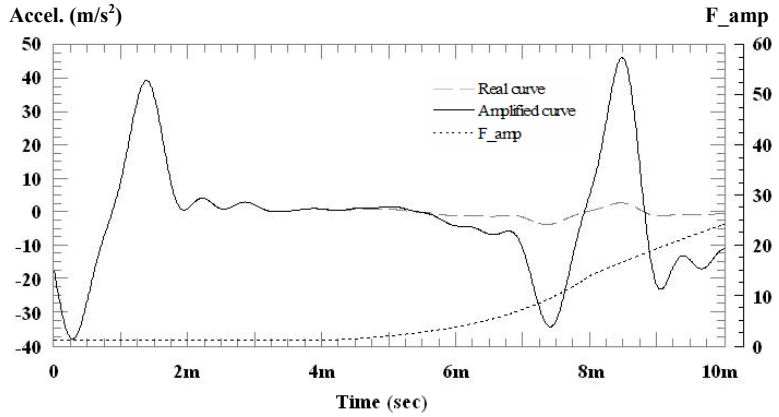

Figure 13 Numerical analysis. Neck defect. 8,000 Hz low-pass filter. Location: 3.25 m

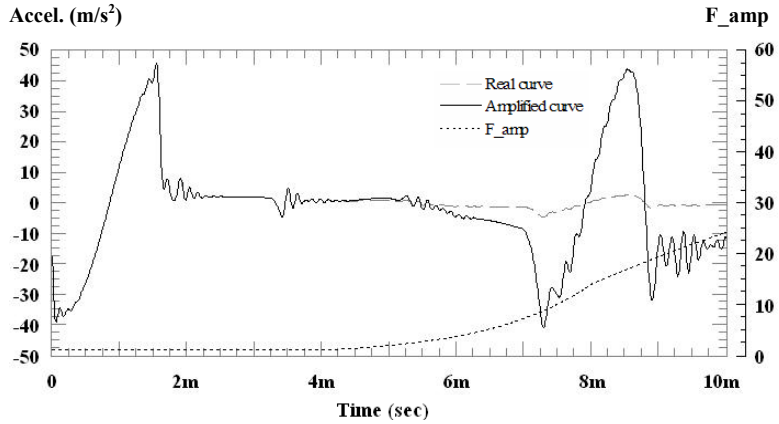

Comparing Figures 12 and 13, it is clear that the defect only is detected when high frequencies are included in the analysis. From a practical point of view, it is very important paying attention to this observation when the accelerometers that would be used in the tests were selected. The frequency range from the accelerometers must cover high frequencies because, in opposite case, defects could pass unnoticed in the analysis.

It must be noted that it is very important the magnitude and duration of the stress pulse induced with the hammer. It would be very difficult to detect a defect located to a distance equal to $V_p \cdot T_p$. For this reason, the impact is better when it introduces high levels of energy in a time as low as possible.

Figure 14 Numerical analysis. Neck defect. 8,000 Hz low-pass filter. Location: 9.75 m

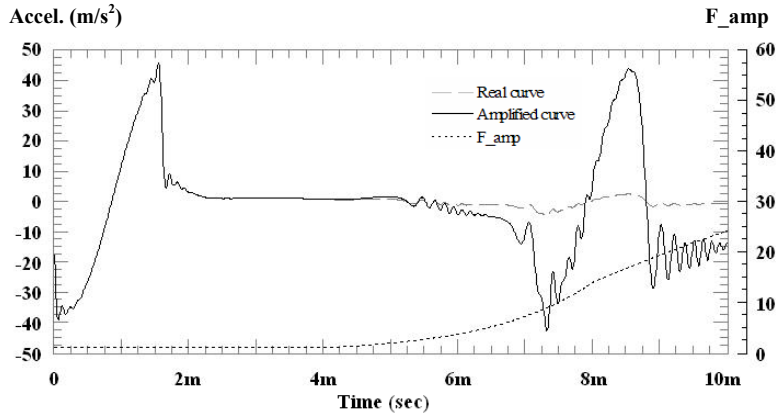

In Figure 14 the dynamic response is presented for a similar neck but located 9.75 m from the head of the pile. It is used the same pulse and an 8,000 Hz low-pass filter. It can be seen that the defect is detected accurately too.

6.3 Bulb defects

In this point, bulb-type defects are analysed. In this case, the bulb diameter (D_b) is 10 cm greater than the diameter of the pile. The other geometrical and physical properties are the same that in point 6.2. In Figure 15, the dynamic response is showed. The accuracy obtained is very good, with an error less than 5%.

Figure 15 Numerical analysis. Bulb defect. 8,000 Hz low-pass filter. Location: 3.25 m

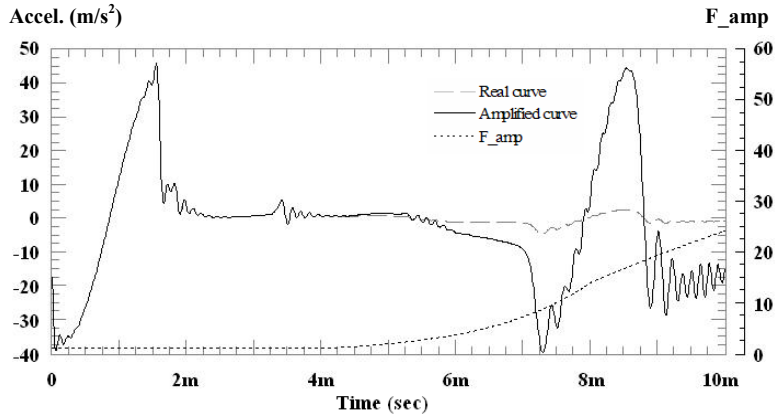

In Figure 16, the dynamic response is presented for bulbs having different lengths: 0.05, 0.1 and 0.2 m. It can be seen a considerable increase in the amplitude of the reflection in the last cases. In Figure 17 the dynamic response for different diameter bulbs is showed: 0.38, 0.43 and 0.48 m. In this case, 0.2 m is adopted as the length of the bulb. Again, it can be seen a considerable increase in the amplitude of the reflection, but it must be

pointed out that it is not possible to distinguish if the defect has greater length or diameter.

Figure 16 Numerical analysis. Bulb defects with different lengths

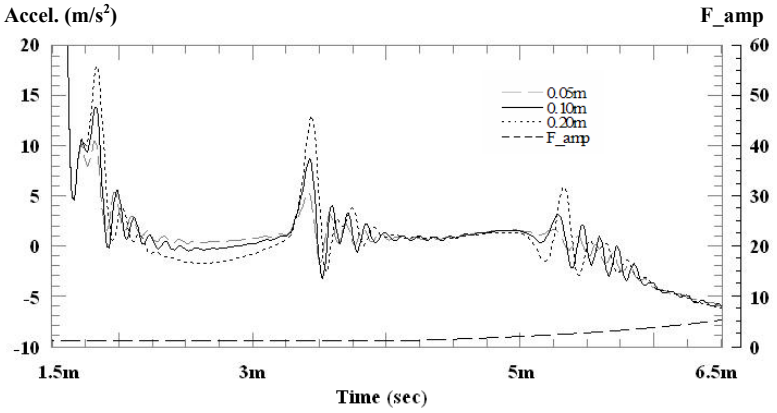

Figure 17 Numerical analysis. Bulb defects with different diameters

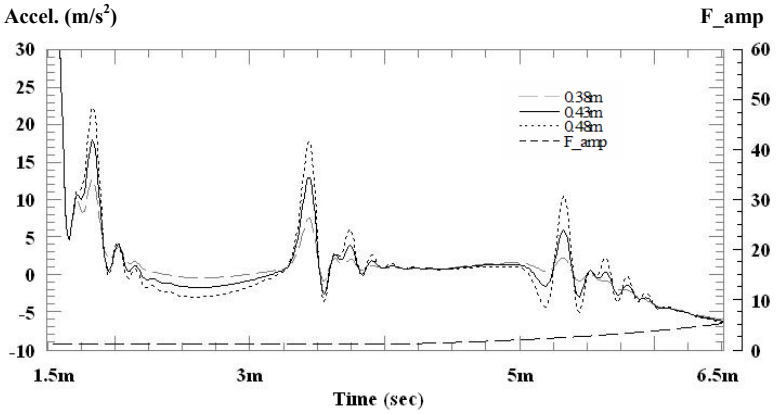

6.4 Neck-bulb defects comparison

It is possible to identify if the defect is neck or bulb type. For this purpose, the boundary condition in a pile is studied. In Figure 18, the dynamic response is presented for a 13 m length and 0.33 m diameter pile with a 3,709 m/s velocity of wave propagation and a 2,400 kg/m^3 mass density. There are two curves corresponding to a fixed-end pile and a pile with a low-stiffness spring similar to a free-end condition one.

Because the elasticity modulus of the soils are lower than concrete (pile), the boundary condition is like a free-end. In this case, taking into account the theory of propagation and reflection of waves in bars, the wave is reflected with the same shape that the impulse. When a neck-type defect exists, there is a weakening of the transverse section and the reflection is like a free-end. When a bulb-type defect exists, the inverse occurs and the reflection is like a fixed-end. This behaviour is observed clearly in Figures 13 to 18.

Figure 18 Numerical analysis. Neck-bulb defect comparison

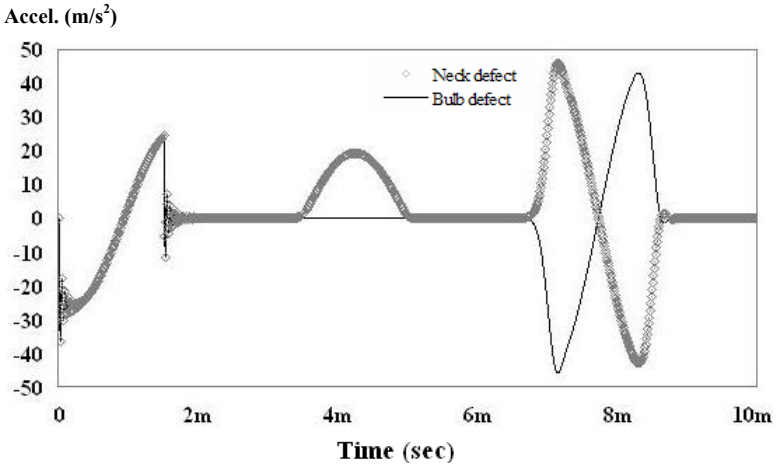

6.5 Influence of the soil properties

Finally, although the soil data were obtained from a reliable database (Segura, 1993), some uncertainties in the soil properties could still remain. Consequently, a numerical study varying the shear modulus of the soil was performed. This soil variable was selected because is the one that has more influence in the global response. A pile with a 13.27 m total length and a free distance of 0.7m is analysed. Moreover, the pulse used has a 13,540 N amplitude and a 1.6 ms total duration. The studied variation of the soil properties is presented in Table 2.

Table 2 Influence of the soil properties

Alternative	*Shear modulus MN/m²*		*Determined length of the pile m*
	Upper layer	*Lower layer*	
Original	3.0	8.0	12.69
1	2.0	6.0	12.67
2	4.0	10.0	12.69

In Figure 19, the responses for the three cases are showed. Moreover, in Table 2, the lengths of the pile obtained for each case are presented.

It can be seen that the qualitative responses are as expected: when the stiffness of the soil increases, the global damping also increases. Moreover, the obtained length of the pile is approximately the same in all cases.

Figure 19 Influence of the soil properties (see online version for colours)

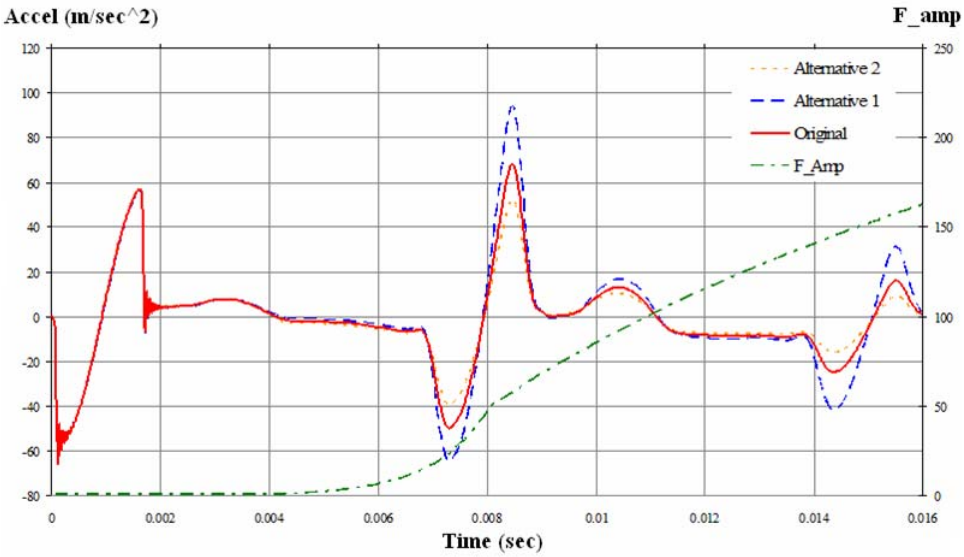

7 Discussion and conclusions

In this paper a dynamic analysis of the integrity of piles with high slenderness ratio in the time domain is presented. The impact-echo method was used and consequently a low-strain impact is applied to send stress waves through the tested element. Then, the superposition of effects and the Hooke's law could be applied. Comparing the theoretical (virgin) and real results, information about the integrity of the pile could be obtained.

Initially, a set of experimental tests with piles isolated in the air were performed. The results in this stage were important to verify some parameters of the numerical model, such as pulse, time step, concrete properties etc.

In the numerical model, the piles were discretised using two-node, isoparametric truss elements in the one-dimensional analysis using standard linear elements under axial deformation, with a linear variation of displacements. To simulate the effect of the soil on the lateral surface of the pile, distributed springs and dashpots were applied to each segment below the ground surface. The soil at the base of the pile was modelled using a spring and a dashpot. The dashpots are intended to represent the radiation (or geometric) damping.

The next stage in the analysis was the study of piles inserted into the soil. Then, similar piles that those studied in the air were tested inserted into the soil. In this case, more differences could be appreciated between the results from experimental tests and the numerical ones. However, taking into account the numerous uncertainties involved, especially with the soil properties, the results are considered satisfactory (differences in pile length between 3–5%). The numerical-experimental comparison allows the calibration of the numerical model.

Finally, neck and bulb-type defects were studied numerically and based in the obtained results; it must be pointed out the following conclusions:

a It could be detected defects with errors minor to 5%.

b Neck and bulb defects could be distinguished.

c In connection with the hammer used, it is very important the magnitude and duration of the stress pulse induced. The impact is better when it introduces high levels of energy in a time as low as possible.

d The use of low-pass numerical filters leads to improvements in the visualisation of results, filtering the high frequency components that generally have lower accuracy. However, the appropriate value of the cut frequency must be analysed carefully in each case because sometimes could exist defects that cannot be detected (see Figures 12 and 13).

e According to the previous conclusion, accelerometers with high frequency range are required. However, it is necessary high sensibility too. Normally, these two properties are opposite.

f The use of amplifying functions in the time domain results invaluable in order to appreciate the reflections in piles inserted into the soil. In this paper, an amplifying function is proposed which combines constant, exponential and logarithmic function. It must be pointed out that the logarithmic function is used for limiting the high grow due to exponential function, which leads to distortions in the signal.

It is important to recognise that, in real-world applications the proposed technique has some limitations, mainly related with the calibration of the amplification function that is fundamental in the procedure. Consequently, it should be important in future works carry out additional experimental tests with piles with known defects. In this sense, it can be said that this paper presents preliminary evidence about the possibility of detect defects in piles with length/diameter relationship up to 40 with the IE technique.

Finally, as it was mentioned in Section 1, it should be emphasised that direct transmission methods are more efficient to detect defects in piles with much larger length but the interest to explore alternatives for the reflection methods is because these methods has low cost and are faster that direct methods.

Acknowledgements

The financial support of CONICET and the University of Tucuman is gratefully acknowledged. Special acknowledgements are extended to the reviewers of the first version of the paper because their useful suggestions led to improvements of the work.

References

Bathe, K.J. (1996) *Finite Element Procedures*, Prentice-Hall, Inc., New Jersey.

Davis, A. and Dunn, C. (1974) 'From the theory to field experience with the non-destructive vibrations testing of piles', *Proc. Instn Civil Eng., Part 2*, Vol. 57, pp.571–593.

Davis, A.G. (2003) 'The nondestructive impulse response test in North America: 1985–2001', *NDT&E International*, Vol. 36, No. 3, pp.185–193.

Duan, J. and Oweis, I. (2005) 'Dyadic wavelet analysis of PDA signals', *Soil Dynamics and Earthquake Engineering*, Vol. 25, Nos. 7–10, pp.661–677.

Ezeberry, J. (2003) *Dynamic Determination of Piles Integrity*, Master Thesis, Structures Intitute, National University of Tucuman, Argentina, in Spanish.

Ezeberry, J., Ambrosini, D. and Danesi, R. (2003) 'Piles defect determination', *XIII Congress About Numerical Methods and Applications*, Argentina, pp.799–813, in Spanish.

Hess, P., Lomonosov, A. and Mayer, A. (2014) 'Laser-based linear and nonlinear guided elastic waves at surfaces (2D) and wedges (1D)', *Ultrasonics*, Vol. 54, No. 1, pp.39–55.

Hewlett-Packard (1998) *HP VEE Advanced Programming Techniques*, Hewlett-Packard Company, USA.

Kim, D., Kim, H. and Kim, W. (2002) 'Parametric study on the impact-echo method using mock-up shafts', *NDT&E International*, Vol. 35, No. 8, pp.595–608.

Kister, G., Winter, D., Gebremichael, Y., Leighton, J., Badcock, R., Tester, P., Krishnamurthy, S., Boyle, W., Grattan, K. and Fernando, G. (2007) 'Methodology and integrity monitoring of foundation concrete piles using Bragg grating optical fibre sensors', *Engineering Structures*, Vol. 29, No. 9, pp.2048–2055.

Li, H., Li, D. and Song, G. (2004) 'Recent applications of fiber optic sensors to health monitoring in civil engineering', *Engineering Structures*, Vol. 26, No. 11, pp.1647–1657.

Liao, S. (1994) *Nondestructive Testing of Piles*, PhD Dissertation, The University of Texas at Austin.

Liao, S. and Roesset, J. (1997) 'Dynamic response of intact piles to impulse loads', *Intern. Journal for Numerical and Analytical Methods in Geomechanics*, Vol. 21, No. 4, pp.255–275.

Liao, S. and Roesset, J. (1997) 'Identification of defects in piles through dynamic testing', *Intern. Journal for Numerical and Analytical Methods in Geomechanics*, Vol. 21, No. 4, pp.277–291.

Liao, S., Tong, J., Chen, C. and Wu, T. (2006) 'Numerical simulation and experimental study of parallel seismic test for piles', *Intern. J. of Solids and Structures*, Vol. 43, Nos. 7–8, pp.2279–2298.

Lilley, D. (2000) 'Integrity testing of pile foundations using axial vibration', *Proc. Instn Civ. Engrs, Geotech Engng*, Vol. 143, No. 4, pp.225–234.

Lin, Y., Sansalone, M. and Carin, N. (1997) 'Impact-echo response of concrete shafts', *Geotechnical Testing Journal*, Vol. 14, No. 2, pp.121–137.

Luo, X., Haya, H., Inaba, T., Shiotani, T. and Nakanishi, Y. (2004) 'Damage evaluation of railway structures by using train-induced AE', *Construction and Building Mater.*, Vol. 18, No. 3, pp.215–223.

Masoumi, H., Degrande, G. and Holeyman, A. (2009) 'Pile response and free field vibrations due to low strain dynamic loading', *Soil Dynamics and Earth. Engn.*, Vol. 29, No. 5, pp.834–844.

Ni, S., Lehmann, L., Charng, J. and Lo, K. (2006) 'Low-strain integrity testing of drilled piles with high slenderness ratio', *Computers and Geotechnics*, Vol. 33, Nos. 6–7, pp.283–293.

Ni, S., Lo, K., Lehmann, L. and Huang, Y. (2008) 'Time–frequency analyses of pile-integrity testing using wavelet transform', *Computers and Geotechnics*, Vol. 35, No. 4, pp.600–607.

Niederleithinger, E. (2012) 'Improvement and extension of the parallel seismic method for foundation depth measurement', *Soils and Foundations*, Vol. 52, No. 6, pp.1093–1101.

Palacz, M. and Krawczuk, M. (2002) 'Analysis of longitudinal wave propagation in a cracked rod by the spectral element method', *Computers & Structures*, Vol. 80, No. 24, pp.1809–1816.

Paquet, J. (1991) 'A new method for testing integrity of piles by dynamic impulse: the impedance log', *International Colloquium on Deep Foundations*, Paris 1991, pp.1–10.

Peeters, B. (2000) *System Identification and Damage Detection in Civil Engineering*, PhD Thesis, Katholieke Universiteit Leuven, Belgium.

Prendergast, L., Hester, D., Gavin, K. and O'Sullivan, J. (2013) 'An investigation of the changes in the natural frequency of a pile affected by scour', *Journal of Sound and Vibration*, Vol. 332, No. 25, pp.6685–6702.

Rao, R. and Rao, N. (1999) 'Dynamics analysis of pile foundations in time – domain using Lanczos vectors', *Computers and Geotechnics*, Vol. 24, No. 4, pp.297–322.

Rausche, F., Goble, G. and Links, G. (1985) 'Dynamic determination of pile capacity', *J Geotech Eng ASCE*, Vol. 111, No. 3, pp.367–83.

Rausche, F., Likins, G. and Ren Kung, S. (1992) 'Pile integrity testing and analysis', *Proceedings of the Fourth International Conference on the Application of Stress-Wave Theory to Piles*, The Netherlands.

Rix, J., Jacobs, L. and Reichert, C. (1993) 'Evaluation of nondestructive test methods for length, diameter and stiffness measurements on drilled shafts. Field performance of structure and nondestructive evaluation of subsurface infrastructure', *Transportation Research Record*, Vol. 1415, pp.69–77.

Segura, F. (1993) *Seismic Micro-Zoning of Tucuman City*, Master Thesis, Structures Institute, National University of Tucuman, Argentina, in Spanish.

Shah, A. and Ribakov, Y. (2010) 'Effectiveness of nonlinear ultrasonic and acoustic emission evaluation of concrete with distributed damages', *Materials & Design*, Vol. 31, No. 8, pp.3777–3784.

Tenenbaum, R., Stutz, L. and Fernandes, K. (2011) 'Comparison of vibration and wave propagation approaches applied to assess damage influence on the behavior of Euler–Bernoulli beams', *Computers & Structures*, Vol. 89, Nos. 19–20, pp.1820–1828.